

Facing the challenge of biosample imaging by FTIR with a synchrotron radiation source

Cyril Petibois,^{a*} Massimo Piccinini,^{b,c} Mariangela Cestelli Guidi^b and Augusto Marcelli^b

^aUniversité de Bordeaux 2, CNRS UMR 5248 CBMN, B8 Avenue des facultés, F-33405 Talence Cedex, France, ^bLaboratori Nazionali di Frascati – INFN, Via E. Fermi 40, 00044 Frascati (Roma), Italy, and ^cPorto Conte Ricerche, SP 55, Porto Conte, Capo Caccia, km 8400, 07041 Alghero (SS), Italy. E-mail: cyril.petibois@u-bordeaux2.fr

Fourier-transform infrared (FTIR) synchrotron radiation (SR) microspectroscopy is a powerful molecular probe of biological samples at cellular resolution (<10 μm). As the brilliance of SR is 100–1000 times higher than that of a conventional Global source, FTIR microscopes are now available in almost all advanced SR facilities around the world. However, in spite of this superior performance, the expected advances in IR SR microscopy have not yet been realised, particularly with regard to bio-analytical studies of single cells and soft tissues. In recent decades solid-state array detectors have revolutionized the fields of molecular spectroscopy and chemical imaging, and now new IR focal plane array detectors implemented at ultra-bright SR facilities will extend the performance and overcome the existing limitations, possibly allowing IR SR instrumentation to achieve the highest sensitivity and resolution of molecular imaging. The impact of IR imaging on large tissue area and the complexity of the analysis are discussed. In view of the high brilliance of SR sources, a comparison of published microscope images is given. Finally, it is briefly outlined how an optimized combination of IR instrumentation and SR optical systems could reach the expected advantages of a SR-based FTIR imaging system.

Keywords: FTIR microscopy; biological tissue; molecular imaging.

1. Introduction

Over the last decade Fourier-transform infrared (FTIR) microscopy has attracted growing interest as being a promising technique for molecular imaging of biological samples. The global molecular information of a sample provided by FTIR analysis is a critical advantage when characterizing biological sample contents (Petibois & Délérès, 2006). This technique is based on the absorption of IR light by vibrational transitions in covalent bonds. In complex systems, such as biological samples, the IR spectrum is the sum of the contributions gathered from all the biomolecules. Furthermore, no internal standard, contrast agent or even staining is required to obtain high-quality spectra from a biological sample. Thus, a wide range of applications could be proposed, from the analysis of individual cells (Ami *et al.*, 2004) to complex tissues (Petibois *et al.*, 2006), and from the characterization of the physiological status of a sample (Malins *et al.*, 2002) to sophisticated disease pattern recognition methods (Fernandez *et al.*, 2005).

However, technical challenges and analytical limitations occur when applying FTIR microscopy to biological issues because of the lack of sensitivity of the detectors while

analyzing thick tissue sections (signal saturation) and, on the other hand, the limited spatial resolution when working on individual cells ($\sim 10 \mu\text{m}$). Hard tissues cannot be easily analyzed owing to their high density of molecular contents at available sample thicknesses, such as for bone or teeth, whose sections are usually thicker than 5 μm , even when diamond saws are used (Mendelsohn *et al.*, 2000). For the same reason, it is not possible to work on soft tissue sections >30–50 μm (Petibois *et al.*, 2006). Analysis of cells requires operation at micrometre (possibly submicrometre) resolution, which is currently impossible with conventional laboratory FTIR instruments. However, opportunities are now offered by a micro attenuated total reflection (ATR) objective combined with a focal plane array (FPA) detector (Chan *et al.*, 2005). Thus, FTIR microscopy may provide sample images with all the molecular information, but its use is still limited to a few biomedical issues of real interest owing to a lack of brilliant sources and/or detector sensitivity. In this context, the use of a synchrotron radiation (SR) source was considered. Its brilliance emission through a 10 μm pinhole is theoretically two to three orders of magnitude higher than that of the conventional Global source found on most FTIR microscopes (Dumas *et al.*, 2007). Thus, because of the superior signal-to-noise ratio

(SNR), the high SR brilliance is expected to guarantee the achievements of spatial resolution down to the diffraction limit, or to make it possible to work on thicker samples while maintaining the ultimate spatial resolution (Smith, 2002). However, although FTIR microscopes became available a decade ago at most of the SR facilities around the world (see <http://www.lightsources.org/cms/>), only a few research studies have quantitatively validated the expected advantages of SR for biomedical issues (Moss *et al.*, 2005; Jamin *et al.*, 1998). A biomedical research effort is running in North America and a large initiative at the European level, named DASIM (Diagnostic Applications of Synchrotron Infrared Microspectroscopy, <http://www.dasim.eu/website.php>), was set up to coordinate the development of this strategic field for future biomedical researches and applications. To date, the main success obtained by combining a FTIR microscope with a SR source has concerned hard-tissue analyses (Huang *et al.*, 2003; Burghardt *et al.*, 2007), which clearly provided results that standard sources could not. Concerning soft-tissue analyses, SR capabilities have not been assessed by systematic studies. Moreover, SR IR microscopy research papers on cells are still very rare compared with those performed with conventional sources (Jamin *et al.*, 1998; Moss *et al.*, 2005). In fact, this discrepancy between the promises of instrumentation which benefits from the superior performance of a SR source and the reasons for the limited performance achieved so far have not been discussed critically.

An accurate evaluation of the performance of SR IR instrumentation is not easy because of the presence, from the source physics to the sample features, of many concurrent experimental contributions that may affect the quality of spectral data. For example, if assessment of the spectral SNR in SR IR microscopy at the diffraction limited resolution is a relevant parameter, it may be significantly affected by SR source instabilities. Moreover, for biological specimens investigated with FTIR instrumentation, few comparisons exist between the use of conventional or SR sources (Petibois *et al.*, 2009). This is notably true for cells or tissues, where the quality of spectra, *e.g.* SNR and image contrast, must be optimized to achieve discriminant analysis and/or recognition of biological relevant parameters. Although in a confocal-like geometry one would expect data of higher quality with a SR source, no quantitative advantages have been clearly addressed.

In this review, the performance of sources and instrumentation is discussed in order to understand the analytical limits of current FTIR microscopy systems and to address possible improvements in SR-based imaging methods for accurate characterization of biological samples.

2. Principles of synchrotron-based FTIR microscopy

Research using SR started at the beginning of the 1960s with pioneering experiments on electron synchrotrons both at Frascati in Italy (1.1 GeV synchrotron) and at the National Bureau of Standards in the USA (180 MeV accelerator) at low energies, *i.e.* with soft X-rays and visible-ultraviolet (V-UV)

radiation. The relevant advance in machine accelerators occurred with the construction of e^+/e^- storage-ring colliders, more stable accelerators designed for high-energy physics. Third-generation light sources, *i.e.* fully dedicated SR storage rings, appeared in the 1980s to host new brilliant and intense light sources owing to insertion devices such as multipole wigglers and undulator magnets (Marcelli, 1996). The features and performance of SR IR beamlines are directly affected by accelerator physics, notably regarding the maximum energy contained in the spectrum of a bending magnet, which is limited by the strength of the magnetic field(s), the minimum radius (curvature) of the particle path, and the energy of the accumulated particles. The formula giving the behaviour of the maximum radiated energy (frequency) as a function of the orbital energy is different from Wien's law describing the behaviour of a black-body thermal source. As temperature changes, the emission of a black body is described by a family of curves that do not have a common limit. By contrast, SR is a non-thermal source whose emission is polarized (in the orbital plane) and described by a family of curves with a characteristic critical energy, all having a common limit at low energy. This particular property is of practical importance because at a fixed wavelength the photons emitted in the IR and visible parts of the spectrum are independent of the orbital energies above 0.5 GeV. Consequently, at IR wavelengths, energy fluctuations owing to instabilities do not affect the photon emission from an accelerator and, as soon as the number of orbiting electrons remains constant, SR is an absolute IR source.

The IR wavelength region of the electromagnetic spectrum is very wide, from 1 to 1000 μm ($10\text{--}10000\text{ cm}^{-1}$), and covered by thermal (standard) sources, such as Globar for the mid-IR or Hg lamps for the far-IR. However, low brilliance is their main limitation. Conversely, SR is a continuous source and all wavelengths are available at the same time for experiments in the entire IR domain, while still keeping the characteristics of high brilliance, natural collimation, polarization and time structure. On the other hand, with respect to thermal sources, SR IR sources suffer from spatial instability. The brilliance indicated above is the photon flux density [$\text{photons s}^{-1}\text{ mA}^{-1}$ ($\text{mrad horizontal})^{-1}$ ($0.1\% \text{ bandwidth})^{-1}$], taking into account the electron beam divergence, the opening radiation angle and the size of the electron beam source [$\text{flux} (\text{mrad vertical})^{-1}\text{ mm}^{-2}$]. The gain in brilliance of IR SR with respect to a Globar source is at least two orders of magnitude.

Considering the unique characteristics of a SR source, it seems evident that IR SR is an indispensable tool for the exploration of matter. The wavelengths of the emitted photons cover a range starting from the atomic level to the biological structures level, *i.e.* up to the micrometre scale. It thus provides unique probes for advanced molecular research on biosamples with good SNR at apertures of a few micrometres (Carr *et al.*, 1995). As addressed above, SR is a non-thermal source and its spectral distribution at low energy (*e.g.* for energy of the accelerated particles much less than the critical energy of the SR source) is the same for all storage rings with an electron beam energy greater than 0.5 GeV, the intensity

being proportional to the circulating current. Consequently, almost all rings are equivalent in terms of IR emission, while beam current and stability can be very different. Both parameters have been significantly improved in recent years and represent the qualifying parameters of an IR SR source. Indeed, an ideal SR source to be used for IR microscopy is an ultra-stable low-energy storage ring operating in topping-up mode, with the highest possible current.

3. Biological studies using SR IR microscopy

FTIR microscopy and imaging techniques achieve contrast *via* the intramolecular vibrational modes, similarly to the well recognized X-ray microscopy methods where contrast is achieved by recording spectra before and after the absorption edges of an element contained in the specimen. The high brilliance of SR makes it easy to reach spatial resolutions of a few micrometres in the mid-IR region, *i.e.* at the diffraction limit with high SNR. In the biological field, IR spectroscopy offers important advantages compared with other techniques: high contrast without staining, the use of non-ionizing radiation and no damage to samples. Whatever the source used, IR radiation is focused through, or reflected from, a tiny spot on the sample and then analyzed with a spectrometer. Although the general optical layout of an IR microscope is always the same, the set-up of a SR IR microscope differs from beamline to beamline owing to the source size, the characteristics of the extraction of the light, the beamline layout, *e.g.* the demagnification of the optical system, the peculiarities of each spectrometer and the microscope objectives.

Experiments performed on individual cells with the use of SR IR microscopy (Holman *et al.*, 2000; Bentley *et al.*, 2007;

Jamin *et al.*, 1998; Heraud *et al.*, 2005) are still very limited. In fact, with a SR IR microscope, single-cell analysis at high spatial resolution is possible (Jamin *et al.*, 1998). If the quality of FTIR spectra obtained by using SR or Globar sources is roughly comparable up to a $10\ \mu\text{m} \times 10\ \mu\text{m}$ aperture, the SNR is very poor below this spatial resolution for the Globar sources (Moss *et al.*, 2005), while it remains useful up to $3\ \mu\text{m} \times 3\ \mu\text{m}$ with the SR sources (Jamin *et al.*, 1998). Thus, a SR source should have an advantage over a thermal source for cell analysis. However, one may wonder about the significance of the spatial resolution parameter for single-cell analysis. In addition, the subcellular components of a eukaryotic cell have a smaller size than those achieved by FTIR microscopy, such as for the nucleus ($1\text{--}3\ \mu\text{m}$), the mitochondria ($\sim 1\ \mu\text{m}$), the ribosomes, podosomes or vesicles ($<1\ \mu\text{m}$) *etc.* Therefore, whether we use SR or conventional IR sources, FTIR images obtained with a $3\ \mu\text{m} \times 3\ \mu\text{m}$ spatial resolution do not probe subcellular components. Thus, unless an ATR objective is used, FTIR microscopy in the mid-IR has actually (significantly) larger lateral resolution than V-UV, X-ray and NMR (Sosnovik & Weissleder, 2007), which all go below $1\ \mu\text{m} \times 1\ \mu\text{m}$. This may explain why applications of SR IR microscopy on cells remain limited. Reasonably, to provide molecular information on subcellular components of cells unavailable by other techniques, the upper limit for the spatial resolution of FTIR microscopy should be about $1\ \mu\text{m} \times 1\ \mu\text{m}$ (Fig. 1).

In the case of imaging performed with spatial resolution below the diffraction limit of the IR light, which is between $10\ \mu\text{m}$ at $1000\ \text{cm}^{-1}$ and $3.3\ \mu\text{m}$ at $3000\ \text{cm}^{-1}$ (the spectral interval of interest for biological samples), it should be noted that the dimensions of the pixel may allow oversampling of the image to dimensions that may be lower than diffraction. Thus,

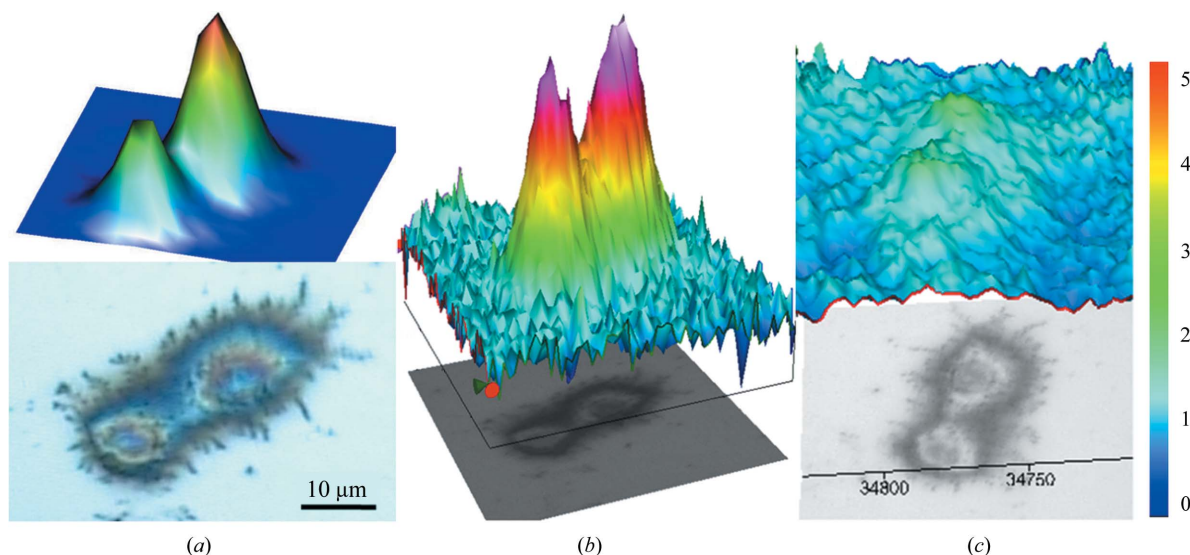


Figure 1

Example of FTIR cell imaging using different spatial resolutions. (a) $6.25\ \mu\text{m} \times 6.25\ \mu\text{m}$ spatial resolution obtained with a Perkin–Elmer Spotlight 300 FTIR imaging system (detector dimension $25\ \mu\text{m} \times 25\ \mu\text{m}$ with a $4\times$ numerical magnification). 64 scans were required to obtain high SNR ($= 1324$), which is sufficient for further data treatments. (b) $2.66\ \mu\text{m} \times 2.66\ \mu\text{m}$ spatial resolution obtained with a Bruker Hyperion 3000 imaging system (detector dimensions $40\ \mu\text{m} \times 40\ \mu\text{m}$ with a $15\times$ numerical magnification). 128 scans were required to obtain sufficient SNR ($= 527$). (c) The same instrumentation as for (b) but with a $36\times$ numerical magnification. The SNR obtained was only 21 and does not permit further spectral data treatment. All FTIR images have been normalized in intensity on a common scale (a.u. of spectrometer) after integration of the $1700\text{--}1600\ \text{cm}^{-1}$ spectral interval (amide I) for every pixel.

data treatment should take into account the dimensions of the pixel *versus* the spectral resolution to avoid artifactual interpretation of the IR image data. Furthermore, interpretation of the results will require that correspondence between visible and IR images features can be verified.

Tissue analysis by SR IR microscopy has achieved the highest performance with hard tissues such as bone (Miller *et al.*, 2001, 2004; Huang *et al.*, 2003; Tobin *et al.*, 2004; Burghardt *et al.*, 2007; Petra *et al.*, 2005; Ruppel *et al.*, 2006) or chondrocytes (Miller *et al.*, 2004), which benefited from the SR brilliance by allowing transmission-mode analyses of thin (4–6 μm) and un-decalcified tissue sections. Comparable results could be obtained using a conventional laboratory system, but with tissue thicknesses between 2 and 4 μm (Boskey *et al.*, 1998; Mendelsohn *et al.*, 2000). Thus, SR allows analysis of bone tissue sections $\sim 50\%$ thicker than Globar sources in transmission mode. However, in this case, the advantage of SR is limited since cutting bone always requires the use of a diamond saw (Miller *et al.*, 2001) and there is no technical difference in sectioning at 2 or 6 μm in thickness. However, it is likely that analysis of a thinner bone tissue section gains in scientific interest, at least because the microstructure of the bone, on the 0.2–1 μm scale, is better resolved. In short, exhaustive comparative studies are still lacking and only a limited number of SR-based FTIR microscopy studies have been able to collect high-quality images on hard tissues.

Studies demonstrating the advantages of using a SR IR sources for analyzing soft tissues are lacking, even more than those for cells and hard-tissue analyses. In fact, regarding conventional FTIR microscopes, thin sample sections allow operation with the best spatial resolution. For most of the biologically relevant questions, the goal is to reach the cell monolayer level, *i.e.* 5 to 6 μm of spatial resolution in the smallest sample volume (voxel) probed in a confocal-like geometry. In this way it will become possible to study cell interactions within tissue morphology, which is critical for studies on pathological processes, drug delivery, blood microenvironment, organ metabolism *etc.* It should also work on very small samples, such as brain exereses or biopsies, *i.e.* on organs which require surgeons to remove the smallest volume containing the largest amount of cells in order to recognize even only a few ‘unhealthy’ cells. In these circumstances, SR may open new applied interface research fields that are almost impossible for academic laboratories to cover, even those equipped with the most modern FTIR systems. Soft-tissues studies using SR may be divided into the FTIR spectroscopy (Wetzel & Williams, 2002; Tobin *et al.*, 2004; Paluszkiwicz *et al.*, 2007; Burghardt *et al.*, 2007; Liu, Zhang *et al.*, 2006) and FTIR microscopy (Szczerbowska-Boruchowska *et al.*, 2007; Miller *et al.*, 2006; Liu, Man *et al.*, 2006) approaches. In the first case, SR is used instead of a ‘classic’ FTIR spectrometer and exploitation of the advantages of the synchrotron source is not an objective *per se*. These studies are usually performed in combination with other techniques such as X-ray fluorescence (Paluszkiwicz & Kwiatek, 2001), also available at synchrotron radiation facilities. Concerning the FTIR imaging microscopy studies, the instrumentation is still

in its infancy so it is too early to validate the advantage of SR over a Globar source, and no systematic imaging studies addressing this aspect have been published yet.

4. Example of soft tissue FTIR microspectroscopy

Since Marcello Malpighi, considered the pioneer of histology in Bologna and Pisa during the 17th century because of his use of the very first optical microscopes, advances in this field have always been in the search for new methods to obtain high contrast between subcomponents of tissues. Analytical methodologies for analyzing soft tissues by IR microscopy are being developed by several research teams around the world (Meier, 2005). As IR spectroscopy is a vibrational technique giving global information about the organic contents of samples, this notion of contrast may be considered as the search for IR absorptions belonging to molecular contents characteristic of the biological subcomponents, *i.e.* subcellular and extracellular parameters. This is a real challenge as tissue samples are more complex than individual cells and the paradox is that most tissue subcomponents diminish the contrast level that spectral data may highlight from their IR microscopy analysis. First, most soft tissues offer only a poor morphological contrast at the macroscopic level, *i.e.* when the tissue area analyzed is multicellular in the three dimensions. At this level, the morphology of cell arrangement must be considered. Second, tissues are made of different cell phenotypes and their three-dimensional spatial arrangement is completely unpredictable. When cell phenotypes are arranged in successive layers, as for skin, the limit between layers is usually imprecisely defined at the microscopic scale. Third, the morphology and molecular contents of cells are comparable for most of the phenotypes, with water content of about 60% (removed for IR microscopy analyses), a phospholipids bilayer (with proteins, cholesterol and polysaccharides), a nucleus (with DNA), ribosomes, a Golgi apparatus, mitochondria and the metabolic machinery (with enzymes and substrates). Fourth, the extracellular components of tissues are primarily built by a few proteinous molecules (collagens), which are notably fibrillar and also arranged in a three-dimensional network.

Therefore, to avoid common IR absorptions in spectra owing to these extracellular components, which would reduce tremendously the potential contrast between tissue subcomponents, the ‘ideal’ situation for IR microscopy analysis should be to work on a ‘unicellular-like’ layer of cells with a spatial resolution that makes it possible to distinguish between cell phenotypes. However, this situation is only marginal in true biology. The main example of cell monolayers highly distinguishable by IR microscopy is found in vascular walls (Petibois & Dél  ris, 2006), which present a monolayer of endothelial cells in the inner part, separated from another one of pericytes in the outer part by a proteinous vascular membrane (Jain, 2003). It is important to note that most of the extracellular layers found in living organisms are due to this kind of proteinous membrane, which is commonly found in connective tissues (epimysium, endomysium and perimysium;

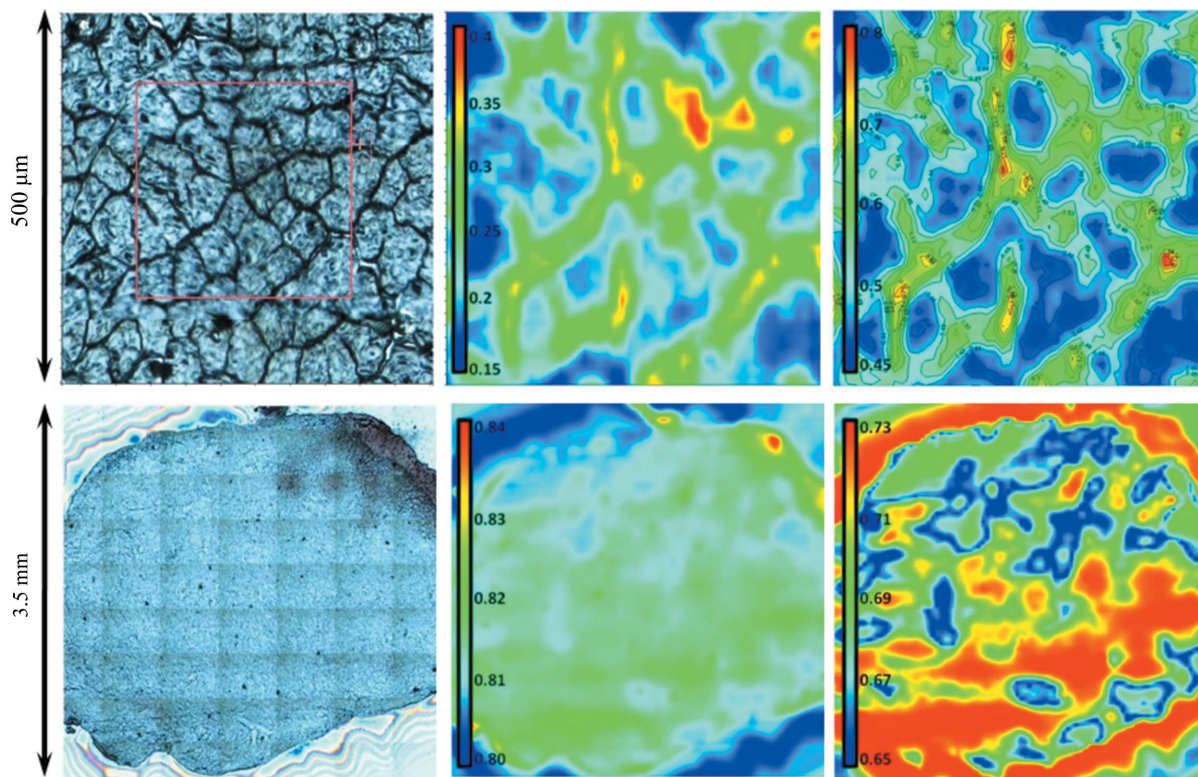


Figure 2

Example of high- and low-contrast IR images from soft tissues. The top series represents visible (left), full spectral intensity (centre; averaged intensity absorption of the $4000\text{--}500\text{ cm}^{-1}$ spectral interval) and lipid/amide ratio (right; intensity absorption of the $1700\text{--}1500\text{ cm}^{-1}$ spectral interval) images of skeletal muscle fibres from fresh tissue ($20\text{ }\mu\text{m}$ section). The red square in the visible image is the area analyzed by FTIR microspectroscopy. The characteristic spatial arrangement of fibres and connective tissue in the muscle allows high-contrast IR images with spectra highlighting the differences in molecular composition to be obtained. The bottom series represents visible (left), full spectral intensity (centre; averaged intensity absorption of the $4000\text{--}500\text{ cm}^{-1}$ spectral interval) and glucose IR absorption (right; distribution of the 1033 cm^{-1} absorption band intensity) images of a rat brain tumor (tissue section of $20\text{ }\mu\text{m}$).

see example of skeletal muscle in Fig. 2) and aponeuroses, but, again, the molecular composition is globally comparable between membrane types. Thus, when these membranes are thick enough ($>1\text{ }\mu\text{m}$) for highlighting the morphology of a tissue, the contrast obtained in images is only at the macroscopic scale. On the other hand, when membranes are thin enough to require microscopic-scale analysis, their composition does not present sufficient heterogeneity to distinguish between membrane types (Belbachir *et al.*, 2009). Thus, again, the contrast level in data is reduced by IR absorptions common to the different spectra. Another issue must be dealt with to allow reproducibility in the analysis of biological tissues: the variability of samples, in terms of morphology as well as molecular composition, owing to the numerous physiological situations an organism may exhibit (healthy or pathologic, starved or fed, male or female, thin or fat *etc.*). Thus, interpretation of spectral data between samples also requires that the internal and external origins of the contrast obtained from tissue subcomponents be distinguished.

Therefore, proposing standardizable analytical methodologies for tissue characterization by IR microscopy will require optimization of pre-analytical steps (tissue thickness, tissue orientation whenever standardizable, reproducibility of physiological situations *etc.*) and post-analytical processes (spectra manipulation, data treatment methods *etc.*). In this

context, the potential gain in spatial resolution and/or in energy owing to the use of SR rather than a Globar source is only one parameter, and this gain cannot be considered as the key factor to succeed in IR microscopic imaging of tissues. Higher spatial resolution will probably enhance tissue subcomponent recognition while analyzing thin tissue sections, probably $<2\text{--}4\text{ }\mu\text{m}$ to avoid cellular and extracellular components superposition. However, at this spatial resolution, and with the available IR flux, such a low tissue thickness of the organic material is actually the lower limit for collecting spectral absorptions. Thus, quantitative analyses are challenging as the specific study of small IR absorptions in highly overlapping spectral intervals (see amide I *versus* amide II bands as an example).

Spatial resolution is certainly a critical parameter in defining the performance of a microscope and evaluating IR microspectroscopy applications. However, as recently pointed out by Carr *et al.* (2001) and Dumas *et al.* (2004), the concept of spatial resolution in IR imaging (discussed in the next section) is not an independent parameter and its definition is associated with the contrast level in the image. In other words, the spatial resolution of an IR image is diffraction-limited; it is affected by the optical design (*e.g.* objectives and apertures) and by the contrast. The contrast in an image is never greater than the contrast in a sample, as the latter is

reduced by the characteristics of the optical system in the middle. Moreover, spatial resolution depends on the wavelength of the light and, as a consequence, the contrast of small features close to the resolution limit is always lower than the contrast of large features. If we combine image contrast and spatial resolution in the unique concept of visibility, this is directly related to the SNR of the image data. Visibility tells us that objects smaller than the diffraction limit are intrinsically associated with lower contrast. Thus more photons are needed to collect images and extract their features from the background. The visibility concept clearly addresses the use of a brilliant IR SR source, the only source capable of delivering the necessary flux on a small-size (*i.e.* $< 10 \mu\text{m}$) sample and still fulfil statistical requirements. The concept is particularly useful when optical aberrations affect the image and/or when we have to resolve small structures in biomedical samples, *e.g.* cells or tissues, which are characterized by different morphology, size and thickness (Lasch & Naumann, 2006).

5. Issues to benefit from SR performances in IR microscopy

5.1. SR IR microscopy performances

The real goal of FTIR microscopy, particularly when using a SR source, is to achieve the best spatial resolution at the sample location, *i.e.* to allow true individual cell imaging at the diffraction limit or below. Single-element MCT detectors optimized in the mid-IR range are characterized by high responsivity and a typical cut-off at 650 cm^{-1} to optimize spectral range and SNR. Then a confocal-like microscope may generate two-dimensional spectral maps with such single-element detectors using an automated sample stage capable of accurate positioning. IR microscopes work with two reflecting-type Schwarzschild objectives to avoid chromatic aberrations. These catoptric lenses are based on two spherical mirrors centred on the same optical axis and allow magnifications of $15\times$ or $36\times$ with numerical aperture (NA) in the range 0.3–0.7. A microscope has a confocal geometry when the two objectives share the same focus at the sample location and both the objective and the collector have a small aperture, placed at the conjugated focus, limiting the illuminated and the detected area on the sample, respectively (Fig. 3).

However, if the use of small pinholes or small rectangular apertures in a microscope allows images to be achieved with a

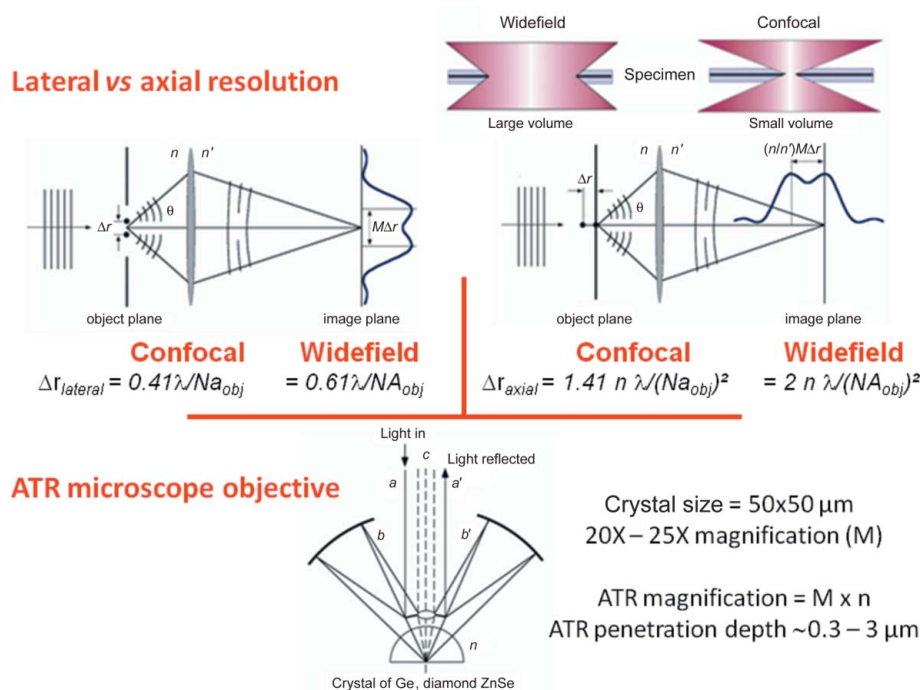


Figure 3

The concept of resolution in FTIR microscopy. Lateral and axial spatial resolution: as clearly shown by equations both the lateral and axial extent of the confocal point spread functions are reduced by $\sim 30\%$ if compared with the corresponding widefield illumination. From the equations it is also underlined that the NA of the microscope objective is much more effective on the axial resolution ($\sim \text{NA}^2$). ATR microscope objective: when a microscope is used in reflection geometry, the incoming radiation illuminates only half the objective aperture and the reflected beam from the specimen returns through the opposite half of the aperture going towards the detector. In the modality of analysis the total magnification of an ATR objective is the product of the magnification of the objective times the refractive index of the internal reflection element (IRE) crystal ($M \times n$) improving the spatial resolution by a factor n . Reflection spectroscopy techniques are also characterized by a small depth of penetration so that a micro-ATR may typically probe depths between ~ 0.3 and $3 \mu\text{m}$. However, the penetration depends also on the wavelength of the radiation, the refractive indices of both specimen and IRE, and by the angle of incidence of the radiation so that, with a degree of control of the penetration, depth-profile studies are possible.

high spatial resolution, the correlated drawback is a very poor photon flux and thus degradation of the SNR in image spectra. Finally, time and spatial resolution are parameters correlated in opposite patterns and thus have to be balanced in order to optimize spectra acquisition with a single-element detector. The metric to monitor and assess both performance and analytical limits is the SNR,

$$\text{SNR} = \text{SP}/\text{NP}, \quad (1)$$

where SP and NP are the source power and the noise power, respectively, both measured in Watts (Smith, 2002). NP can be determined using the formula

$$\text{NP} = (A_d/t)^{1/2}/D^*, \quad (2)$$

where A_d is the detector area and D^* is the specific detectivity. Considering the source power as constant, the SNR increases as the noise power decreases, *i.e.* it increases by reducing the detector area and/or increasing its detectivity. The typical size of a single-element detector ranges between $50 \mu\text{m} \times 50 \mu\text{m}$ and $100 \mu\text{m} \times 100 \mu\text{m}$ to better match the standard apertures of IR for microscopes working with conventional sources.

Conversely, working with a conventional source at high lateral resolution ($\leq 10 \mu\text{m} \times 10 \mu\text{m}$), *e.g.* with apertures smaller than the detector area, the SNR strongly decreases because a significant reduction in photon flux may be monitored and the detector noise remains constant. In fact, neglecting possible non-linear contributions, if we consider a detector of area $100 \mu\text{m} \times 100 \mu\text{m}$ with a microscope aperture of $10 \mu\text{m} \times 10 \mu\text{m}$, the IR flux illuminating the detector is reduced by two orders of magnitude while its noise remains constant. In this case, even working with a SR source, whose brilliance is two to three orders greater than a standard IR source, will not change the SNR significantly at spatial resolutions much smaller than the detector size.

To overcome this limitation, several projects are under way to test and align MCT detectors with smaller area ($\sim 10 \mu\text{m} \times 10 \mu\text{m}$) to take advantage of their reduced electronic noise. These latter systems, with pixel size typically ranging from $6.25 \mu\text{m}$ to $25 \mu\text{m}$, may replace conventional single-element detectors, but their spatial resolution is determined by the optics of the entire system and they do not require apertures.

Because the source size of a non-thermal SR source is naturally small, radiation is emitted in a narrow angular range ($\sim \text{mrad}$), allowing a high throughput by small aperture sizes. Indeed, the high brilliance of the synchrotron source allows smaller regions with acceptable SNR, *e.g.* $\sim 10 \mu\text{m}$ area (or lower), to be sampled, while it provides limited advantages over a thermal source for moderate apertures ($>20 \mu\text{m}$) and no advantages for large apertures ($>70 \mu\text{m}$). Comparison of the throughput between a SR and a Globar source *versus* the

aperture size clearly shows that a Globar source has weak transmission through a $10 \mu\text{m}$ aperture, whereas $>80\%$ of the synchrotron IR light passes through the same size aperture (Miller & Dumas, 2006) (Fig. 4).

As a consequence, although they have not been designed for these sources, SR-based FTIR microscopy systems perform well owing to the higher brilliance of the SR source and the lack of thermal noise. In particular, the available spatial resolution previously limited by the brilliance becomes diffraction-limited, a condition associated with apertures defining a region comparable with or smaller than the wavelength of the light (Carr *et al.*, 2001; Dumas *et al.*, 2004).

Particularly for a confocal layout, the experimental throughput tells us how good the optical coupling is between the beamline and the microscope itself. In a real optical layout, a slight misalignment of one (or more) of the optical elements of the beamline may introduce at the sample location, *e.g.* at 10–20 m from the source, aberrations and inhomogeneous illumination at the entrance of the interferometer. The spot gives rise to unmatched working conditions for the whole instrumental system, but more significantly for the microscope, and thus a strong reduction in the photon flux on the detector and in image quality.

5.2. The spatial resolution issue in IR microscopy

As discussed above, with a ‘true’ confocal microscope an IR spectrum is collected using two apertures, one placed before and one placed after the sample, to be representative of a

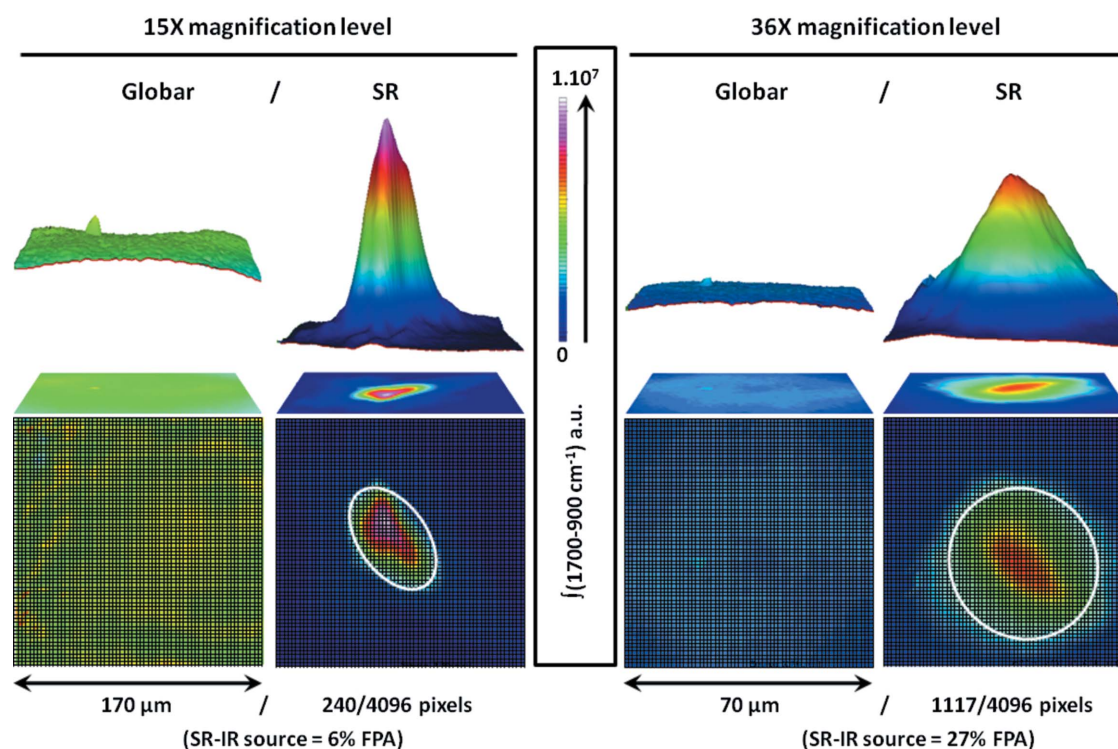


Figure 4 Schematic drawing of thermal and SR IR sources alignment features on a FTIR imaging system equipped with a FPA detector. A higher magnification level ($36\times$ *versus* $15\times$) induces a loss in detector illumination by one order of magnitude whatever the source considered, but SR covers much more of the detector for its brightest part, thus enhancing the SNR. Images were obtained at the DAFNE Light Laboratory at the Laboratori Nazionali di Frascati, Italy.

small area with negligible contributions from the non-illuminated part of the sample. In fact, a test based only on the SNR ratio of the 100% line is insufficient because energy from outside the sample area may reach the detector and contribute to the signal. Considering the optical system and the wavelength of the probing radiation, the aperture(s) plays an important role in defining the effective spatial resolution of an instrument. The resolution of a microscope is the mathematical relationship between the specimen and the collected image, *e.g.* the convolution. At the simplest level, the convolution is the relation existing between a small point of the illuminated object and its blurred image. The spatial resolution is the minimum distance d required to collect the spectra at two points on the specimen, neglecting the contribution from its nearest neighbour. The spatial resolution depends on the microscope illumination (Fig. 3). A wide-field microscope objective focuses a wide cone of radiation over a large volume of a uniformly illuminated specimen. In this geometry the signal is affected significantly from areas and volumes above and below the focal plane with a reduction in both resolution and contrast of the image. In a confocal microscope, the light is focused by the objective to a very small spot at the focal plane and the image is obtained by a raster scan of the specimen. The spatial resolution of an infrared microscope as defined by the diffraction limit is quite well described by $2\lambda/\text{NA}$, *i.e.* from three to four times the wavelength depending on the NA of the instrument. However, it is clear that a trade-off between spatial resolution, wavelength, SNR and collection time exists, and certainly the latter is a relevant parameter in image processes because it is associated with sample dynamics and dose, notably in biology.

In order to roughly evaluate the experimental capabilities, the theoretical optimum spatial resolution of a confocal-like IR microscope is about λ/NA and measurements performed with standard resolution targets or with a knife-edge confirmed that the spatial resolution of an imaging system is governed by both wavelength and NA. Combining a confocal-like microscope with a SR source, the spatial resolution may be increased at least up to $\sim\lambda/2$, *i.e.* down to the diffraction limit. However, the diffraction limit is only one of the parameters to consider while determining the experimental spatial resolution of far-field microscopy. In addition, mirror objective, shape and size of apertures, and detector geometry and size all contribute to the effective spatial resolution as determined by source brilliance and sample characteristics. Nevertheless, recent detailed spatial resolution tests have demonstrated that the source contribution on the demagnified spot on the microscope stage does not significantly affect a mid-IR image and, as expected, the spatial resolution limit of $\sim 0.5\ \mu\text{m}$ can be achieved at a wavelength around $1\ \mu\text{m}$ (Levenson *et al.*, 2008).

The limited spatial resolution for mid-IR analyses might be overcome by collecting the evanescent wave emitted by the surface of a sample put at the contact of an ATR objective, and the imaging mode should be allowed by coupling it to a FPA detector. In an ATR objective, the flat surface of an internal reflection element (IRE) crystal is placed at the focal

plane of the reflecting microscope objective. A magnified image of the specimen is seen when the specimen is pressed against the flat surface of the IRE crystal. An ATR objective works with three modalities: survey, contact and analysis, so that the technique measures a specimen placed in optical contact with the surface of an IRE. When the IR beam enters an IRE crystal at the critical angle, internal reflection occurs. Few materials are optimal IRE crystals because we need (large) homogenous crystals with a high refractive index and, in addition, materials have to be transparent throughout the largest mid-IR region and capable of withstanding the physical and chemical contact with different types of specimens (the characteristic refractive index of IRE materials at $5\ \mu\text{m}$: Ge = 4; diamond IIa = 2.39; GaAs = 3.82; Ge = 4.02; Si = 3.42; ZnSe = 2.43). The development of ATR objectives made it possible to extend infrared reflection spectroscopy (IRS) to imaging at micrometre and submicrometre spatial resolutions.

Nowadays, ATR-FTIR is a well established technique applied mainly to the study of hard, thick or opaque samples. When this technique is used, the radiation propagates in a high-index-of-refraction IRE and the same radiation interacts with a sample characterized by a lower refractive index. At the interface a non-propagating evanescent wave penetrates the surface of the sample to a depth of the order of the wavelength of the radiation. With an ATR objective, higher spatial resolution microspectroscopy images than in transmission geometry can be achieved. The increased magnification is approximately given by the refractive index (n) of the IRE material, and is associated with the experimental conditions. Indeed, the sample is immersed in a medium with a higher index of refraction and as a consequence the already diffraction-limited spot generated by microscope optics is additionally reduced by the factor n .

Using an ATR objective with an IR microscope increases both the spatial and volumetric resolutions because the evanescent wave can be collected with a $1\ \mu\text{m} \times 1\ \mu\text{m}$ to $2\ \mu\text{m} \times 2\ \mu\text{m}$ spatial resolution and for $1\ \mu\text{m}$ to $3\ \mu\text{m}$ in the z -axis of soft-tissue samples, depending on the ATR crystal used. A germanium crystal ($n = 4$) allows sample absorption to be collected in the first micrometres with an optimal signal from the first 300 nm. With a diamond crystal ($n = 2.4$), $3\ \mu\text{m}$ of the sample thickness can be probed, with an optimal absorption collection in the first micrometre (Fig. 3). Thus, with a 64×64 pixels FPA detector, one can expect to collect the evanescent wave from the sample surface for a $100\ \mu\text{m} \times 100\ \mu\text{m}$ area, *i.e.* an area greater than the size of an individual cell. Moreover, by using a 128×128 pixel FPA detector, a $200\ \mu\text{m} \times 200\ \mu\text{m}$ area might be covered in imaging mode.

This permits relevant biological applications for tissue analyses, notably for cancer because these dimensions correspond to those of small tumors or metastases which are hardly detectable with other imaging methods. Several beamlines are currently testing this promising approach, which might combine the necessary spatial resolution for cell analyses with the greater potential of SR, compared with conventional sources. As outlined above, in an ATR experiment we can control the optical path length, and, maybe in the future, by

combining materials with different refractive indexes, which allow different penetration depths, the ability to reconstruct three-dimensional FTIR images even on thin biological sections will become possible.

The last concept dealing with spatial resolution in IR microspectroscopy is that lateral spatial resolution is associated with a resolution criterion, *i.e.* the ability to record the separation of two closely spaced objects inside a sample. As an example, in the Rayleigh criterion two points can be separated when the central maximum of the first Airy disc is placed at a distance of just one radius. However, this criterion is valid only when the signal associated with the two points has the same intensity, a condition that corresponds to a minimum contrast of 26.4%. As a consequence, independently of the criterion selected to define the lateral resolution, the latter is only a parameter whose relationship with the contrast is fundamental in determining the resolving power of a microscope. Moreover, the correlation between lateral resolution and contrast in a sample can be described by the modulation (or contrast) transfer function (MTF) of the imaging system, which is a function that depends on the spatial frequency. The MTF explains why the contrast in an image may not be the same as that for the sample and thus how the imaging optical system degrades the contrast level as a function of spatial frequency. In fact, the contrast of small features just inside the resolution limit is much lower than that of larger structures.

5.3. SR instabilities in IR microscopy

Considering equation (1), SNR is the effective parameter to monitor in order to achieve an optimal FTIR spectrum. The result may be obtained by maximizing the source power and/or minimizing the noise power. Regarding sources, significant work can be done by trying to optimize the different components: brilliance of the electron source, solid angle acceptance and optical parameters (*e.g.* NA and/or demagnification factors). Optimization of these parameters might determine a gain of more than one order of magnitude at many different facilities.

In parallel, for microscopy analysis of small-size samples, the practical advantage of the SR IR source brilliance is limited by instabilities of the source that affect the reproducibility of the spectral data and SNR. The instabilities may concern the electron beam position, its transverse dimension and its angular deviation with respect to the standard orbit, which affect the transmission performance of a beamline (Cestelli-Guidi *et al.*, 2005). While working with SR, current instabilities and decay over time may significantly affect the brilliance and the reproducibility of spectra in both a short- and a long-term period, *i.e.* from seconds to minutes. The problem may be critical for the acquisition of spectral images, which are a function of the time scale for large-spectrum collection. Beam instabilities have been detected in most storage rings but are sometimes difficult to understand and fix. Moreover, a few synchrotron radiation facilities introduced the topping-up mode, which is a continuous refill procedure that is extremely useful for SR experiments as it provides

practically an infinite beam lifetime. However, unavoidable beam instabilities during injections and refilling are still detected in IR microscopy applications, strongly suggesting dedicated operation for high-resolution IR imaging.

5.4. The FPA solution

The availability of IR FPA detectors, two-dimensional arrays of small IR detectors allowing the acquisition of thousands of IR spectra simultaneously, revolutionized laboratory-based IR imaging systems using conventional IR sources. FPA detectors allow much more than chemical and spatial information to be obtained from a single hyper-spectral data set. Imaging techniques based on FPAs were originally developed for remote sensing for military purpose and later applied in astronomical applications. Only in the early 1990s were the first IR spectroscopic applications considered. Spectral images collected with FPAs are three-dimensional blocks of data that span one wavelength and two spatial dimensions. The spectroscopic resolution is defined by the number of wavelength readout elements, *e.g.* bands or channels, while the spatial resolution at a fixed wavelength is determined by the size of the pixel and the parameters of the optical system (Miller & Smith, 2005). The major gain in performance with FPA detectors is that the IR image of an area is obtained within minutes, when previously hours were necessary with single-element IR microscopes.

Since the first IR detector appeared in the 1990s, important advances have been made in terms of pixel numbers, low noise and faster readout, so much so that now several companies offer FPA-based IR imaging systems. A microscope equipped with a FPA does not need apertures, thus the optical system is not confocal and generating a small focal spot at the sample is not required. On the contrary, the focal spot has to be expanded to cover the area imaged by the FPA, apparently reducing the brilliance advantage of a SR IR source. Modern arrays can match a brilliant IR source with a moderate expansion of the beam maintaining the high SNR characteristic of SR emission. The first experiments that matched a FPA IR detector (64×64) with synchrotron radiation were successfully performed at ANKA in 2005. Although an aperture-free imaging system does not reach the ultimate resolution of a confocal dual-aperture optical set-up and the spectral range of these detectors is limited with respect to single-element MCT detectors, both are, however, sufficient for the majority of FTIR microscopy experiments. In this context, the installation of FPA detectors for IR spectral imaging has been performed or is being tested with different spectrometers in most IR SR facilities.

Confocal-like single-element mapping is the method that allows the highest spatial resolution compared with apertureless imaging systems such as a FPA system, particularly when dealing with extremely brilliant SR sources. However, not all experiments need the ultimate resolution and, as addressed by recent experimental data (Moss *et al.*, 2006), SR emission is characterized by sufficient photon flux density capable of illuminating the array detector in order to operate

with a high SNR. Furthermore, when using high magnification levels, such as $36\times$ or even $74\times$, aligning a single ‘small-size’ detector with the objective of a confocal-like IR microscope may be very difficult owing to the instability of SR IR sources. As an example, a $40\ \mu\text{m} \times 40\ \mu\text{m}$ detector with a $74\times$ magnification level on the microscope will give a final pixel size of about $0.5\ \mu\text{m} \times 0.5\ \mu\text{m}$. As a SR IR source usually has a diameter of about $20\ \mu\text{m}$ with an instability of a few micrometres at its brightest part, it is impossible to maintain a constant photon flux over hours if a sample image has to be acquired (typically $30\ \mu\text{m} \times 30\ \mu\text{m}$ for an individual cell, thus 60×60 pixels with $2\ \text{minutes pixel}^{-1}$). On the contrary, a FPA with 64×64 detectors covers a $2.5\ \text{mm} \times 2.5\ \text{mm}$ area, which becomes $35\ \mu\text{m} \times 35\ \mu\text{m}$ with a $74\times$ magnification level. As all image FTIR spectra are acquired at the same time, the fluctuation of the photon flux on each pixel is reduced with respect to a confocal-like microscope set-up.

Thus, FPA detectors allow images to be collected significantly faster than point-by-point measurements. For example, a $p \times p$ pixel FPA detector may provide up to a p^2 time-saving compared with a single-element detector, *e.g.* if $p = 64$, more than three orders of magnitude, readout well beyond 1 kHz and noise characteristics similar to single-element detectors. Experiments performed with conventional instrumentation have clearly shown that, by combining the sensitivity and the speed of readout of last-generation FPAs, the time may scale down from hours to minutes (Petibois & Dél  ris, 2006). Thus, by using FPAs with SR sources it will be possible to minimize the illumination conditions among spectral data obtained in sequence by IR microscopy instrumentation while beam current decreases *versus* time and/or between two contiguous refills. Except on the most modern storage rings where almost continuous refill occurs, in standard accelerators injections are performed from tenths of minutes to hours while the current continuously decreases. For IR beamlines, instabilities are one of the main issues to investigate, particularly when working with FPA detectors as they contain thousands of pixels, *e.g.* 64×64 or 128×128 pixels are typically used, and for these devices it is mandatory to work with signal uniformity over the entire field of view. Using a standard IR source, the noise in imaging is mainly spatial, *i.e.* working in a standard FTIR imaging configuration the different noise contributions are typically lower than the FPA detector noise (Bhargava & Levin, 2001). SR instabilities may introduce a not negligible contribution of temporal noise that, when combined with the spatial noise and other additional contributions coming from optics and electronics, may significantly affect the SNR and introduce wavelength-dependent variations in the signal. Thus, a thermal source still maintains a clear advantage over a SR source when FTIR imaging is performed with a FPA detector. The example of SR IR source alignment on the FPA detector of the FTIR imaging system illustrated in Fig. 4 shows the importance of magnification level for allowing the SR IR source to cover the maximum of FPA detectors. With the $36\times$ magnification level, the pixel dimension in the final IR image is about $1\ \mu\text{m} \times 1\ \mu\text{m}$, thus well below the diffraction limit for the mid-IR range, but 35% of pixels are covered. Conversely,

the use of a $15\times$ magnification level reduces the FPA coverage to only 11% of detectors for a $2.6\ \mu\text{m} \times 2.6\ \mu\text{m}$ pixel size in the final IR image. The counterpart to this lower FPA coverage by the SR IR source is that the IR image becomes very noisy (most of the detectors have no IR signal, thus only noise, and averaged SNR decreases). Finally, the choice is between the respect of diffraction limit considering the pixel size of the final IR image *versus* the level of noise acceptable for interpreting IR spectra.

At present, at diffraction-limited wavelengths, the spatial resolution of images collected by FPAs illuminated by SR sources is mainly limited by the physical pixel size. In the future, even in this aperture-less system, thanks to the high SNR available with SR it will be possible to introduce a multiple aperture mask at an intermediate image plane, reaching the ultimate spatial resolution of the confocal-like layout. Using high spatial oversampling methods a resolution enhancement by point spread function (PSF) deconvolution could also be achieved. Deconvolution of experimental images is a well known procedure substantially obtained by employing the PSF of the optical system, together with the Fourier self-deconvolution method largely applied to resolve overlapped IR bands in IR spectroscopy. Both can be applied to increase the spatial resolution in IR images, although other techniques exist, such as image-compression algorithms. The latter methods, reading only the relevant subset of pixels and removing redundant information, may achieve images with subdiffraction-limited resolution and faster data acquisition (Gallet *et al.*, 2008).

Finally, a detailed spatial resolution analysis for SR-based IR spectromicroscopy was reported in a recent work (Levenson *et al.*, 2008). In order to set the spatial resolution limit at different wavelengths for a definite SR source, the study addressed the contribution of electron beam size and the parameters specific to an IR beamline, *e.g.* demagnification of beamline optics, demagnification of microscope objectives and NA. In particular, the spatial resolution is significantly affected by the NA of the microscope objective, which is a parameter that measures its angular capability to collect radiation. In the future, improvements are expected on infinity-corrected catoptric objectives with large NAs to combine the advantage of a SR source while working well below the diffraction limit spatial resolution.

6. Conclusions

A decade of efforts has underlined the technological challenge of coupling IR instruments to SR sources. It is worth noting that the coupling of IR microscopes to SR IR beamlines is still at an early stage of development rather than in a routine application phase. Today, efforts are being devoted to installing and commissioning detectors or linear arrays of small-size detectors in IR microscopes to improve the optical system performances. As an alternative to the pure confocal geometry, which is not available at present, the use of FPA detectors optimized in the mid-IR range appears to be the best way to collect fast IR images over large areas because of the

sensitivity and readout speed. However, the alignment and optimization of these detectors on commercial systems remains a challenge owing to optical limitations and when SR noise and/or instabilities are present. A huge effort has already been made, many ideas have been implemented and others are under investigation at third-generation storage ring facilities in order to improve stability and, as a consequence, imaging performance, in terms of spatial resolution, contrast and acquisition time. There is thus a 'brilliant' future for IR SR microscopy and imaging. The SR advantages exist and, thanks to the continuously improving performance of these light sources, important results are expected in biological and biomedical applications in the near future. The future of FTIR imaging, not only FPA imaging, is however, correlated with the development of powerful multivariate data analysis procedures. To manage large hyper-spectral data sets, new and accurate methods have to be developed to simultaneously analyze and correlate spatial and spectral information. New deconvolution methods and compressive imaging procedures are available and will be used in the years to come in order to improve the spatial resolution and, thanks also to the excellent readout performance of the modern FPAs, obtain faster imaging.

The authors are indebted to Miss Carolyn Kent for her support in the redaction of this manuscript, and to the Association Française contre les Myopathies (AFM) and Ligue Nationale Contre le Cancer for financial support.

References

- Ami, D., Natalello, A., Zullini, A. & Doglia, S. M. (2004). *FEBS Lett.* **576**, 297–300.
- Belbachir, K., Noreen, R., Gouspillou, G. & Petibois, C. (2009). *Anal. Bioanal. Chem.* **385**, 829–837.
- Bentley, A. J., Nakamura, T., Hammiche, A., Pollock, H. M., Martin, F. L., Kinoshita, S. & Fullwood, N. J. (2007). *Mol. Vision*, **13**, 237–242.
- Bhargava, R. & Levin, I. W. (2001). *Anal. Chem.* **73**, 5157–5167.
- Boskey, A. L., Gadaleta, S., Gundberg, C., Doty, S. B., Ducy, P. & Karsenty, G. (1998). *Bone*, **23**, 187–196.
- Burghardt, A. J., Wang, Y., Elalieh, H., Thibault, X., Bikle, D., Peyrin, F. & Majumdar, S. (2007). *Bone*, **40**, 160–168.
- Carr, G. L., Kramer, S. L., Murphy, J. B., Lobo, R. P. S. M. & Tanner, D. B. (2001). *Nucl. Instrum. Methods Phys. Res. A*, **463**, 387–392.
- Carr, G. L., Reffner, J. A. & Williams, G. P. (1995). *Rev. Sci. Instrum.* **66**, 1490–1492.
- Cestelli-Guidi, M., Piccinini, M., Marcelli, A., Nucara, A., Calvani, P. & Burattini, E. (2005). *J. Opt. Soc. Am. A*, **22**, 2810–2817.
- Chan, K. L. A., Kazarian, S. G., Mavraki, A. & Williams, D. R. (2005). *Appl. Spectrosc.* **59**, 149–155.
- Dumas, P., Jamin, N., Teillaud, J. L., Miller, L. M. & Beccard, B. (2004). *Faraday Discuss.* **126**, 289–302; 303–211.
- Dumas, P., Sockalingum, G. D. & Sule-Suso, J. (2007). *Trends Biotechnol.* **25**, 40–44.
- Fernandez, D. C., Bhargava, R., Hewitt, S. M. & Levin, I. W. (2005). *Nat. Biotechnol.* **23**, 469–474.
- Gallet, J., Riley, M., Hao, Z. & Martin, M. C. (2008). *Infrared Phys. Technol.* **51**, 420–422.
- Heraud, P., Wood, B. R., Tobin, M. J., Beardall, J. & McNaughton, D. (2005). *FEMS Microbiol. Lett.* **249**, 219–225.
- Holman, H.-Y. N., Martin, M. C., Blakely, E. A., Bjornstad, K. & McKinney, W. R. (2000). *Biopolymers*, **57**, 329–335.
- Huang, R. Y., Miller, L. M., Carlson, C. S. & Chance, M. R. (2003). *Bone*, **33**, 514–521.
- Jain, R. K. (2003). *Nat. Med.* **9**, 685–693.
- Jamin, N., Dumas, P., Moncuit, J., Fridman, W. H., Teillaud, J. L., Carr, G. L. & Williams, G. P. (1998). *Proc. Natl. Acad. Sci. USA*, **95**, 4837–4840.
- Lasch, P. & Naumann, D. (2006). *Biochim. Biophys. Acta*, **1758**, 814–829.
- Levenson, E., Lerch, P. & Martin, M. C. (2008). *Infrared Phys. Technol.* **51**, 413–416.
- Liu, C., Zhang, Y., Yan, X., Zhang, X., Li, C., Yang, W. & Shi, D. (2006). *J. Lumin.* **119–120**, 132–136.
- Liu, K. Z., Man, A., Shaw, A., Liang, B., Xu, Z. & Gong, Y. (2006). *Biochem. Biophys. Acta*, **1758**, 960–967.
- Malins, D. C., Hellstrom, K. E., Anderson, K. M., Johnson, P. M. & Vinson, M. A. (2002). *Proc. Natl. Acad. Sci. USA*, **99**, 5937–5941.
- Marcelli, A. (1996). *Proceedings of the International School of Physics E. Fermi on Biomedical Applications of Synchrotron Radiation*, Course CXXXVIII, edited by E. Burattini, pp. 21–45. Varenna: SIF.
- Meier, R. J. (2005). *Chem. Soc. Rev.* **34**, 743–752.
- Mendelsohn, R., Paschalis, E. P., Sherman, P. J. & Boskey, A. L. (2000). *Appl. Spectrosc.* **54**, 1183–1191.
- Miller, L. M. & Dumas, P. (2006). *Biochim. Biophys. Acta*, **1758**, 846–857.
- Miller, L. M., Novatt, J. T., Hamerman, D. & Carlson, C. S. (2004). *Bone*, **35**, 498–506.
- Miller, L. M. & Smith, R. J. (2005). *Vibrat. Spectrosc.* **38**, 237–240.
- Miller, L. M., Vairavamurthy, V., Chance, M. R., Mendelsohn, R., Paschalis, E. P., Betts, F. & Boskey, A. L. (2001). *Biochim. Biophys. Acta*, **1527**, 11–19.
- Miller, L. M., Wang, Q., Telivala, T. P., Smith, R. J., Lanzirotti, A. & Miklossy, J. (2006). *J. Struct. Biol.* **155**, 30–37.
- Moss, D., Gasharova, B. & Mathis, Y.-L. (2006). *Infrared Phys. Technol.* **49**, 53–56.
- Moss, D. A., Keese, M. & Pepperkok, R. (2005). *Vibrat. Spectrosc.* **38**, 185–191.
- Paluszkiwicz, C. & Kwiatek, W. M. (2001). *J. Mol. Struct.* **565–566**, 329–334.
- Paluszkiwicz, C., Kwiatek, W. M., Banas, A., Kisiel, A., Marcelli, A. & Piccinini, M. (2007). *Vibrat. Spectrosc.* **43**, 237–242.
- Petibois, C. & Délérís, G. (2006). *Trends Biotechnol.* **24**, 455–462.
- Petibois, C., Deleris, G., Piccinini, M., Cestelli Guidi, M. & Marcelli, A. (2009). *Nat. Photon.* **3**, 179.
- Petibois, C., Gionnet, K., Goncalves, M., Perromat, A., Moenner, M. & Délérís, G. (2006). *Analyst*, **131**, 640–647.
- Petra, M., Anastassopoulou, J., Theologis, T. & Theophanides, T. (2005). *J. Mol. Struct.* **733**, 101–110.
- Ruppel, M. E., Burr, D. B. & Miller, L. M. (2006). *Bone*, **39**, 318–324.
- Smith, T. D. (2002). *Nucl. Instrum. Methods Phys. Res. A*, **483**, 565–570.
- Sosnovik, D. E. & Weissleder, R. (2007). *Curr. Opin. Biotechnol.* **18**, 4–10.
- Szczerbowska-Boruchowska, M., Dumas, P., Kastyak, M. Z., Chwiej, J., Lankosz, M., Adamek, D. & Krygowska-Wajs, A. (2007). *Arch. Biochem. Biophys.* **459**, 241–248.
- Tobin, M. J., Chesters, M. A., Chalmers, J. M., Rutten, F. J., Fisher, S. E., Symonds, I. M., Hitchcock, A., Allibone, R. & Dias-Gunasekara, S. (2004). *Faraday Discuss.* **126**, 27–39; 77–92.
- Wetzel, D. L. & Williams, G. P. (2002). *Vibrat. Spectrosc.* **30**, 101–109.